JETIR.ORG ISSN: 2349-5162 | ESTD Year : 2014 | Monthly Issue
JOURNAL OF EMERGING TECHNOLOGIES AND INNOVATIVE RESEARCH (JETIR)
An International Scholarly Open Access, Peer-reviewed, Refereed Journal

MHD Flow of an Oscillatory Rotating Newtonian Fluid over a Vertical Plate with First-Order Slip Flow Regime in Porous Medium

Babul Chandra Das[1], Dr. Mira Das[2]

[1]Department of Mathematics, Research Scholar, Mahapurusha Srimanta Sankaradeva Viswavidyalaya (MSSV), Nagaon – 782436, Assam, India.

[2]Department of Mathematics, Assistant Professor, Mahapurusha Srimanta Sankaradeva Viswavidyalaya (MSSV), Nagaon – 782436, Assam, India.

ABSTRACT:
This study investigates the magnetohydrodynamic (MHD) flow of electrically conducting fluids through porous media of an oscillatory flow of Newtonian fluid past a vertical plate subject to a first-order velocity-slip boundary condition. Particular attention is given to the influence of key governing parameters, including the heat absorption parameter (Q), chemical reaction parameter (α), thermal radiation parameter (Nr), Prandtl number (Pr), and Schmidt number (Sc). The effects of the thermal and mass Grashof numbers (Gr) and (Gc) on the velocity field (q), as well as the effects of (Sc) and (α) on the concentration distribution (C), are systematically analysed. By invoking the boundary-layer approximations, the coupled governing equations are transformed into a dimensionless system of ordinary differential equations and solved numerically using MATLAB. The numerical results demonstrate that magnetic and rotational effects exert substantial control over the velocity distribution and boundary-layer characteristics, thereby influencing the hydrodynamic stability of the flow. The incorporation of the first-order slip condition produces notable modifications in the velocity field near the plate. The results provide valuable insight into the coupled heat and mass transport mechanisms in oscillatory rotating MHD flows and may contribute to a better understanding of transport phenomena in systems involving slip at solid boundaries.

Keywords: MHD; Newtonian fluid; Oscillatory flow; Rotating fluid; Slip flow.

1. Introduction:

Magnetohydrodynamic (MHD) flow of electrically conducting fluids through porous media has received considerable attention because of its importance in numerous engineering and industrial applications, including geothermal systems, petroleum extraction, nuclear reactors, polymer processing, metallurgical operations, cooling systems, and energy conversion devices. The interaction between an electrically conducting fluid and an applied magnetic field significantly modifies the momentum transport through the generation of Lorentz forces. When such flows occur in a porous medium, the resistance offered by the porous matrix introduces an additional mechanism that influences the velocity and temperature distributions. The combined effects of magnetic fields and porous resistance therefore provide a useful framework for describing many practical transport phenomena.

The study of unsteady flow over vertical surfaces is particularly important because oscillating boundaries can produce time-dependent momentum and thermal boundary layers. In many practical situations, the surface may oscillate periodically, while the surrounding fluid is simultaneously subjected to buoyancy forces, magnetic effects, heat transfer, and mass diffusion. Das and Das [1] investigated an unsteady MHD flow of a viscous, incompressible, electrically conducting fluid over an oscillating vertical surface embedded in a Darcian porous regime. Their analysis incorporated rotation, heat generation or absorption, and thermal radiation, demonstrating the significant influence of these physical mechanisms on the transport characteristics. Similarly, Pal and Talukdar [7] examined MHD radiating heat and mass transfer in a Darcian porous regime bounded by an oscillating vertical surface, highlighting the importance of unsteadiness, radiation, and porous resistance in coupled heat and mass transport.

Rotation introduces additional complexity into MHD boundary-layer flows because the Coriolis force modifies the momentum equations and couples the velocity components. Rotating flows over oscillating vertical plates are therefore of considerable theoretical and practical interest. Singh et al. [2,7] studied the influence of Hall and ion-slip currents on unsteady MHD free-convective flow of a rotating fluid past an oscillating vertical plate. Their work illustrates that, in addition to the primary magnetic interaction, modifications of the electrical conductivity characteristics of the fluid can substantially alter the flow and heat-transfer behaviour. Rotational effects have also been investigated in porous channels. Ahmed [3] considered Hartmann Newtonian radiating MHD flow in a rotating vertical porous channel immersed in a Darcian porous regime and obtained an exact solution. This study is particularly relevant to models involving Newtonian fluids, magnetic fields, rotation, thermal radiation, and Darcy resistance.

Heat transfer in porous media is further affected by the thermal characteristics of the fluid and the boundary conditions imposed at the solid-fluid interface. In conventional no-slip models, the velocity of the fluid at the wall is assumed to coincide with the velocity of the surface. Thermal slip can likewise modify the temperature gradient and consequently the rate of heat transfer. Ganesh et al. [4] investigated heat transport of a Newtonian fluid in a porous medium with quadratic-order thermal slip, demonstrating the relevance of non-classical thermal boundary conditions in porous-media transport. Jasim [5] also examined MHD flow with slip boundary conditions, showing the usefulness of analytical approaches for problems involving magnetic effects and wall slip. Furthermore, studies of peristaltically induced MHD slip flow in porous media [10] provide useful mathematical treatments for incorporating slip conditions into MHD porous-flow models.

Much attention has been given to this type of fluid flow problem with various physical effects via both analytical and numerical techniques [8]. Nandeppanavar et al. [12] studied the quadratic order velocity slip with heat transfer in a viscous fluid. A closed form analytical solution was presented for the momentum equation and the energy equation was solved numerically in [12]. Turkyilmazoglu [13] derived the analytical solution for MHD viscous fluid ow using Laguerre polynomials with quadratic order velocity slip. Mabood et al. [15] also studied on radiation effects on stagnation point flow with melting heat transfer and second order slip. Liu et al [14], Aman et al. [15]. In the above articles, a closed form solution for momentum equation was presented and the energy equation was solved using confluent hyper-geometric function. Numerous numerical investigations on the fluid flow with quadratic order velocity slip. Recently, Ganesh et al. [17] have carried out a numerical investigation on the Newtonian fluid over a vertical stretching sheet with quadratic order velocity and thermal slip boundary condition. Having all the above literature in mind, we focused in this communication on the problem of Newtonian fluid ow over a stretching sheet immersed in a porous medium with suction.

Motivated by the above studies, the present investigation considers the unsteady MHD flow and heat-transfer characteristics of a Newtonian electrically conducting fluid adjacent to an oscillating vertical surface embedded in a Darcian porous medium. The formulation incorporates the effects of rotation, thermal radiation, porous-medium resistance, and appropriate slip boundary conditions. The governing momentum and energy equations are formulated by accounting for the relevant physical forces and thermal transport mechanisms, and the resulting problem is investigated to determine the influence of the governing dimensionless parameters on the velocity and temperature fields as well as the associated engineering quantities. Particular attention is given to the interaction between magnetic effects, rotational forces, Darcy resistance, oscillatory motion, radiation, and slip parameters. The results are expected to provide useful theoretical insight into coupled MHD transport in rotating porous systems.

The flow occurs past a vertically moving plate embedded in a porous medium within a rotating system. The analysis considers the effects of first-order velocity slip, Hall current, thermal radiation, chemical reaction, and the Soret effect. This paper is especially relevant to Das, et al. [1].

1.1 *Formulation of Governing Equations:*

The flow diagram is a physical model for the unsteady incompressible, viscous electrically acting micropolar fluid. The Newtonian fluid particles that allow to rotate independently of the overall flow. the flow is over an infinite moving vertical surface and rotating with a first order slip flow regime. The x-axis is the vertical direction along the plate and the direction normal(perpendicular) to the plate.

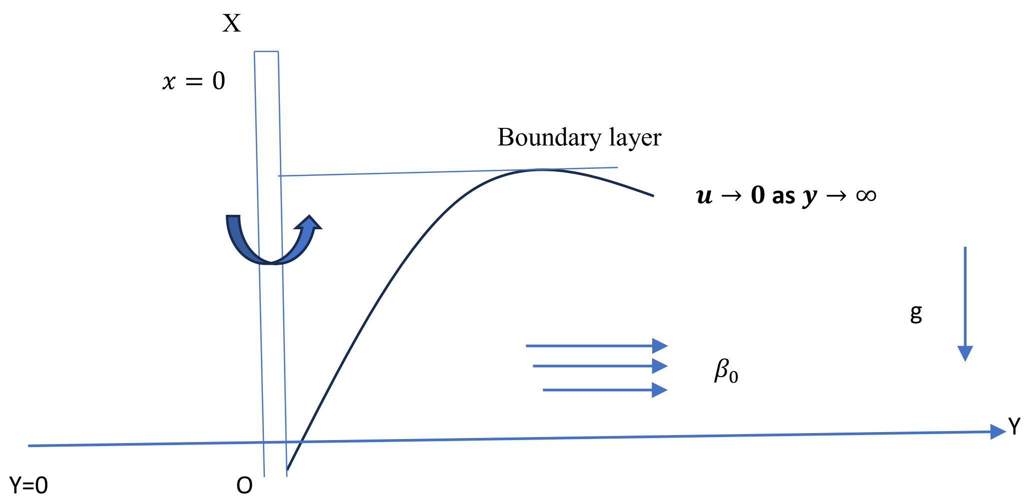

Let v_0 be the section velocity at the plate, then the flow variables are function of y^* and the t^*.

A Uniform magnetic field (β_0) is applied transversely (along the y axis). the Circular arrow signifies that the entire system is rotating about the vertical axis i.e. the influence of angular velocity Ω. The equation of continuity then gives $v = V_0$ everywhere in the fluid where V_0 is the section velocity at the plates.

$$\frac{\partial v^*}{\partial y^*} = 0 \tag{1}$$

$$\frac{\partial u^*}{\partial y^*} + v^*\frac{\partial u^*}{\partial y^*} - 2\Omega w^* = \gamma\frac{\partial^2 u^*}{\partial y^{*2}} + g\beta_T(T^* - T^*_\infty) + g\beta_c(C^* - C^*{}_\infty) - \frac{\gamma u^*}{K^*} + \frac{\alpha\beta_0^2(m\omega^* - u^*)}{\rho(1+m^2)} \tag{2}$$

$$\frac{\partial \omega^*}{\partial t^*} + v^*\frac{\partial \omega^*}{\partial y^*} + 2\Omega u^* = \gamma\frac{\partial^2 \omega^*}{\partial y^{*2}} - \gamma\frac{\alpha\beta_0^2(\omega^* - mu^*)}{\rho(1+m^2)} - \frac{\gamma\omega^*}{K^*} \tag{3}$$

$$\rho C_p\left(\frac{\partial T^*}{\partial t^*} + v^*\frac{\partial T^*}{\partial y^*}\right) = \frac{\partial^2 T^*}{\partial y^{*2}} - \frac{\partial q_r}{\partial y^*} - Q_0(T - T_\infty) \tag{4}$$

$$\frac{\partial C^*}{\partial t^*} + v^*\frac{\partial C^*}{\partial y^*} = D_M\frac{\partial^2 C^*}{\partial y^{*2}} - K_C^*(C^* - C^*{}_\infty) \tag{5}$$

With boundary conditions

$$q = q_p + A\frac{\partial q}{\partial \eta}, \theta = e^{i\omega t}, C = e^{i\omega t} \text{ at y=0}$$

$$q \to 0, \theta \to 0, C \to 0 \text{ at y} \to \infty \tag{6}$$

Following the Rosseland approximation, the relative heat flux is

$$q_r = -\frac{4\sigma^*}{3K_1^*}\frac{\partial T^{*4}}{\partial y^*} \tag{7}$$

Assuming that the differences in temperature within the flow are such that T^{*4} can be expressed as a linear combination of the temperature T^*,and neglecting the higher order terms of $(T^* - T_\infty)$, we have

$$T^{*4} = -3T_\infty^4 + 4T_\infty^3 \tag{8}$$

Introduce the following dimensionless quantities:

$$u = \frac{u^*}{V_0}, v = \frac{v^*}{V_0}, w = \frac{w^*}{V_0}, \eta = \frac{V_0 y^*}{\vartheta}, t = \frac{t^* V_0}{4\vartheta}, \omega = \frac{4\vartheta\omega^*}{V_0^2}$$

$$\theta = \frac{T^* - T_\infty^*}{T_w^* - T_\infty^*}, C^* = \frac{C^* - C_\infty}{C_w^* - C_\infty^*}, j = \frac{V_0^2 j}{\vartheta^2}, U_p = \frac{u_p^*}{V_0}, w_p = \frac{w_p^*}{V_0} \tag{9}$$

Substituting equation (9) into equation (2)-(6) and using (1), (7), (8) yields the following non-dimensional equation:

$$\frac{1}{4}\frac{\partial u}{\partial t} - \frac{\partial u}{\partial \eta} - Rw = \frac{\partial^2 u}{\partial \eta^2} + G_r\theta + G_c C - \frac{M}{(1+m^2)}(mw + u) - \frac{u}{K} \tag{10}$$

$$\frac{1}{4}\frac{\partial w}{\partial t} - \frac{\partial w}{\partial \eta} + Ru = \frac{\partial^2 w}{\partial \eta^2} - \frac{M}{(1+m^2)}(w - mu) - \frac{w}{K} \tag{11}$$

$$\frac{1}{4}\frac{\partial \theta}{\partial t} - \frac{\partial \theta}{\partial \eta} = \frac{1}{Pr}(1 + Nr)\frac{\partial^2 \theta}{\partial \eta^2} - \frac{Q}{Pr}\theta \tag{12}$$

$$\frac{1}{4}\frac{\partial C}{\partial t} - \frac{\partial C}{\partial \eta} = \frac{1}{Sc}\frac{\partial^2 C}{\partial \eta^2} - \alpha C \tag{13}$$

The boundary condition becomes

$$q = q_p + A\frac{\partial q_0}{\partial \eta}, \theta = e^{i\omega t}, C = e^{i\omega t} \text{ at } y = 0$$

$$q_0 \to 0, \theta_0 \to 0, C_0 \to 0 \text{ at } y \to \infty \tag{14}$$

Where

$$A = \frac{L_1 V_0}{\vartheta}, B = \frac{L_2 V_0^2}{\vartheta^2}, \beta = \frac{\vartheta_r}{\vartheta}, Nr = \frac{16 T_\infty^3 \sigma^*}{3K_1^* k}, M = \frac{\sigma \beta_0^2 \theta}{\rho V_0^2}, Pr = \frac{\rho C_p \vartheta}{k}, Sc = \frac{\vartheta}{D_M}, R = \frac{2\vartheta\Omega}{V_0^2},$$

$$Gr = \frac{g\vartheta\beta_T(T_w^* - T_\infty^*)}{V_0^2}, Gc = \frac{g\vartheta\beta_c(C_w^* - C_\infty^*)}{V_0^2}, \alpha = \frac{2\Omega\vartheta}{V_0^2}, Q = \frac{4\vartheta Q^*}{V_0^2}, K = \frac{V_0^2 K^*}{\vartheta^2}$$

The equation (10) – (11), by introducing $q = u + iw$ can be written as

$$\frac{1}{4}\frac{\partial q}{\partial t} - \frac{\partial q}{\partial \eta} + iRq = \frac{\partial^2 q}{\partial \eta^2} - \frac{M}{(1+m^2)}(1 - im)q + Gr\theta + GcC - \frac{q}{K} \tag{15}$$

$$\frac{1}{4}\frac{\partial \theta}{\partial t} - \frac{\partial \theta}{\partial \eta} = \frac{1}{Pr}(1 + Nr)\frac{\partial^2 \theta}{\partial \eta^2} - \frac{Q}{Pr}\theta \tag{16}$$

$$\frac{1}{4}\frac{\partial C}{\partial t} - \frac{\partial C}{\partial \eta} = \frac{1}{Sc}\frac{\partial^2 C}{\partial \eta^2} - \alpha C \tag{17}$$

The boundary condition (14) becomes

$$q = q_p + A\frac{\partial q_0}{\partial \eta}, \theta = e^{i\omega t}, C = e^{i\omega t} \text{ at } y = 0$$

$$q_0 \to 0, \theta_0 \to 0, C_0 \to 0 \text{ at } y \to \infty \tag{18}$$

After using non-dimensional

1.2 *Method of Solution:*

To solve the equation (9)-(17), we assume

$$q = q_0(\eta)e^{i\omega t}, \theta = \theta_0(\eta)e^{i\omega t}, C = C_0(\eta)e^{i\omega t} \tag{19}$$

Using (19), then the equation (15) to (17) becomes

Equation (15) becomes,

$$\Rightarrow q_0'' + q_0' - a_1 q_0 = -Gr\theta_0 - GcC_0 \tag{20}$$

Where $\frac{1}{K} + \frac{iw}{4} + \frac{M(1-im)}{(1+m^2)} = a_1$

Equation (16) becomes

$$\Rightarrow a_2\theta_0'' + \theta_0' - a_3\theta_0 = 0 \tag{21}$$

Similarly, equation (17) becomes

$$\Rightarrow \mathrm{C}_0'' + \mathrm{ScC}_0' - \mathrm{Sca}_4\mathrm{C}_0 = 0 \tag{22}$$

The corresponding boundary condition becomes

$$q = q_p + A\frac{\partial q_0}{\partial \eta}, \theta = e^{i\omega t}, C = e^{i\omega t} \text{ at } y = 0$$

$$q_0 \to 0, \theta_0 \to 0, C_0 \to 0 \text{ at } y \to \infty \tag{23}$$

The solution of the equation (20)-(22) with the boundary condition (23) is obtained as

$$\theta = e^{i\omega t - m_2\eta} \tag{24}$$

$$C = e^{i\omega t - m_3\eta} \tag{25}$$

$$q = (Ee^{i\omega t} - E_2)\eta \tag{26}$$

The Local skin friction co-efficient (C_f) is given by

$$C_f = -q'(0) = -(E_1e^{i\omega t} - E_2) = E_2 - E_1e^{i\omega t} \tag{27}$$

The rate of heat transfer at the surface in terms of the Nusselt number (Nu) is given by

$$NuRe_x^{-1} = -\theta'(0) = -(-m_2e^{i\omega t}) = m_2e^{i\omega t} \tag{28}$$

The rate of mass transfer at the surface of the local Sherwood number is given by

$$ShRe_x^{-1} = -C'(0) = -(-m_3e^{i\omega t}) = m_3e^{i\omega t} \tag{29}$$

2. Results and Discussion:

Figures 1–7 present the velocity profiles for different values of the thermal Grashof number (Gr), solutal Grashof number (Gc), magnetic parameter (M), Prandtl number (Pr), heat absorption parameter (Q), Schmidt number (Sc), and chemical reaction parameter (α). Figures 8–9 illustrate the concentration profiles corresponding to variations in (Sc) and (α), respectively, while Figures 10–12 show the temperature profiles for different values of (Q), (Pr), and radiation parameter (Nr).

Figure 1 shows the velocity profile (q) against the similarity variable η for ($Gr = 1,2,3$). Increasing (Gr) enhances the velocity near the plate, with ($Gr = 3$) producing the maximum velocity. This behaviour is attributed to the strengthening of thermal buoyancy forces. However, the profiles gradually converge as (η) increases, indicating that the influence of (Gr) becomes weaker away from the plate.

Figure 2 shows that the heat-transfer parameter decreases with η. Increasing (Gc) slightly enhances heat transfer near the plate, while its influence diminishes in the outer region.

Figure 3 indicates that the heat-transfer parameter decreases with η. Higher (M) suppresses heat transfer by opposing fluid motion, with its effect becoming negligible away from the surface.

Figure 4 demonstrates that the heat-transfer parameter decreases with increasing η, while higher (Pr) produces a steeper decline, indicating reduced thermal diffusivity and a thinner thermal boundary layer.

Figure 5 shows that velocity decreases from its maximum near the plate toward the outer region. Increasing (Q) reduces the velocity by strengthening heat absorption and weakening buoyancy-driven momentum transport.

Figure 6, illustrates the distribution of the dimensionless concentration q against the similarity variable η for Schmidt numbers $Sc = 0.66,0.60.0.30$. The concentration is highest at the wall and decays smoothly with increasing η, approaching zero in the far-field region, which reflects diffusion-controlled mass transport. A reduction in the Schmidt number increases mass diffusivity, leading to higher concentration values and an expanded concentration boundary layer. Hence, the profile corresponding to $Sc = 0.30$ lies above those for $Sc = 0.60$ and $Sc = 0.66$ throughout the domain.

Figure 7, represents the distribution of the dimensionless concentration q with respect to the similarity variable η for chemical reaction parameter values $\alpha = 0,0.5.1$. The concentration begins at its highest level at the surface and decreases smoothly as η increases, approaching zero in the outer region of the flow. It is evident that stronger chemical reactions lower the concentration within the boundary layer by accelerating species depletion. Accordingly, the non-reactive case maintains higher concentration levels than those observed for moderate and strong reaction parameters throughout the domain.

Figure 8, seen that the variation of the dimensionless concentration C with the similarity variable η for Schmidt numbers $Sc = 0.66, 0.60, 0.30$. The concentration starts from its maximum value at the surface and decreases smoothly with increasing η, tending to zero in the outer flow region. It is evident that decreasing the Schmidt number increases mass diffusion, which leads to higher concentration levels and an expanded concentration boundary layer. As a result, the profile for $Sc = 0.30$ remains above those for $Sc = 0.60$ and $Sc = 0.66$ throughout the domain.

Figure 9, shows the dimensionless concentration C as a function of the similarity variable η. The concentration is highest at the surface and decreases steadily with increasing η, approaching zero far from the surface, indicating the development of a concentration boundary layer. The curves show the effect of a controlling parameter on mass transfer. Higher values of this parameter reduce the concentration across the boundary layer, resulting in a thinner layer due to increased diffusion or faster species consumption near the surface.

Figure 10, observed that the variation of the dimensionless temperature θ with the similarity variable η for heat absorption parameter values $Q = 0, 0.5, 1$. The temperature is highest at the surface and decreases steadily with increasing η, approaching the ambient state in the far-field region. An increase in the heat absorption parameter lowers the temperature within the boundary layer by strengthening energy removal from the fluid. As a result, the case $Q = 0$ exhibits higher temperature levels than those corresponding to $Q = 0.5$ and $Q = 1$ throughout the flow region.

Figure 11 shows that the dimensionless temperature decreases with (η), with higher (Pr) producing a sharper decline due to reduced thermal diffusivity and a thinner thermal boundary layer.

Figure 12 demonstrates that increasing (Nr) elevates the temperature within the boundary layer, thereby increasing its thickness through enhanced radiative heat transfer.

Table 1 summarizes the effects of (Pr), (Nr), heat generation, and rotation on the reduced Nusselt number ($NuRe_x^{-1}$). Increasing (Pr) enhances $NuRe_x^{-1}$, whereas higher (Nr) reduces it by weakening the wall-temperature gradient. Heat generation significantly modifies the heat-transfer rate, while rotation has only a marginal effect within the considered range.

Table 2 presents the variation of the Sherwood number with the governing parameters. Increasing the chemical reaction parameter reduces the Sherwood number, whereas the rotation parameter has a negligible effect. In contrast, increasing the Schmidt number enhances ($ShRe_x^{-1}$), indicating stronger mass transfer at the plate surface.

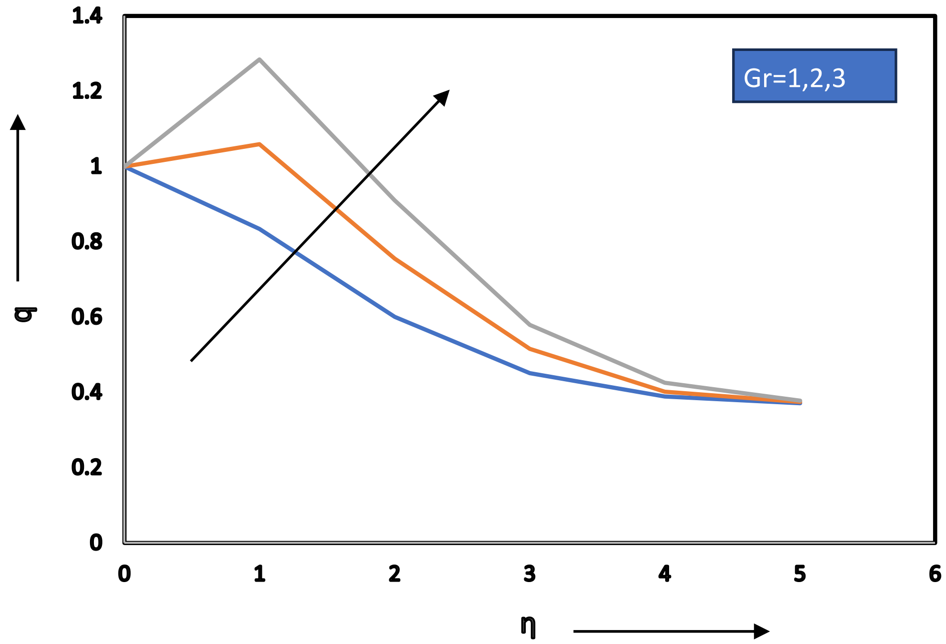

Figure1: Variation of velocity for Gr

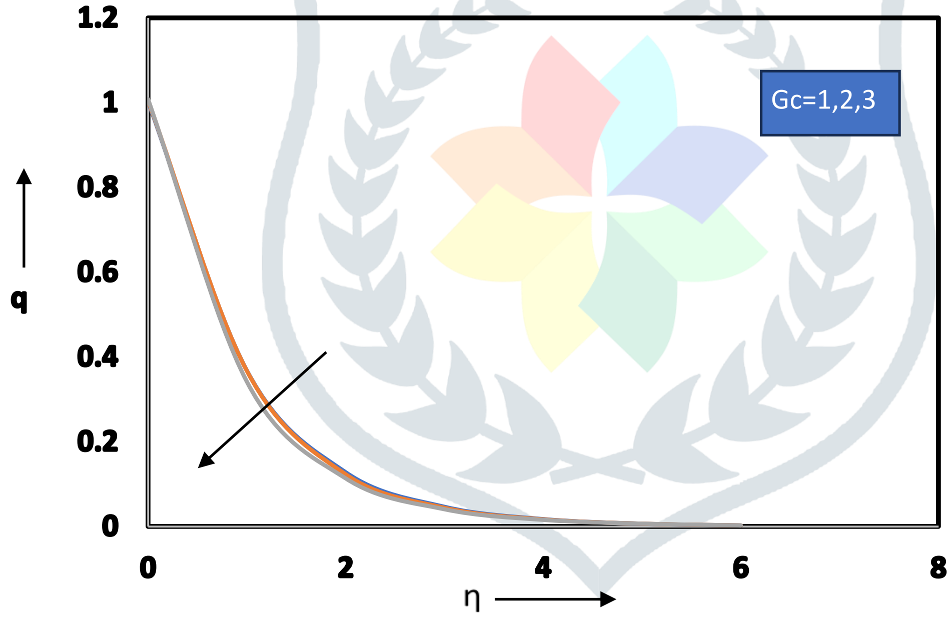

Figure 2: Variation of velocity for Gc

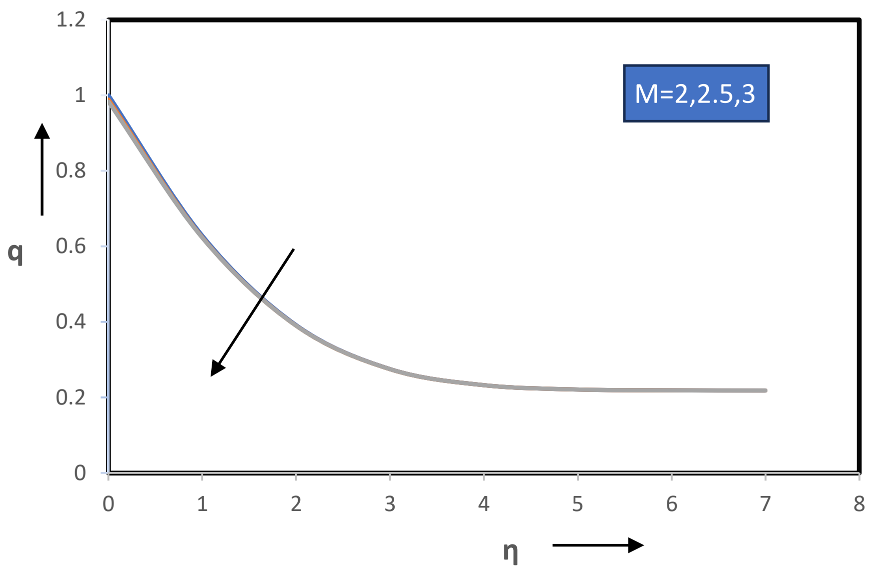

Figure 3: Variation of velocity for M

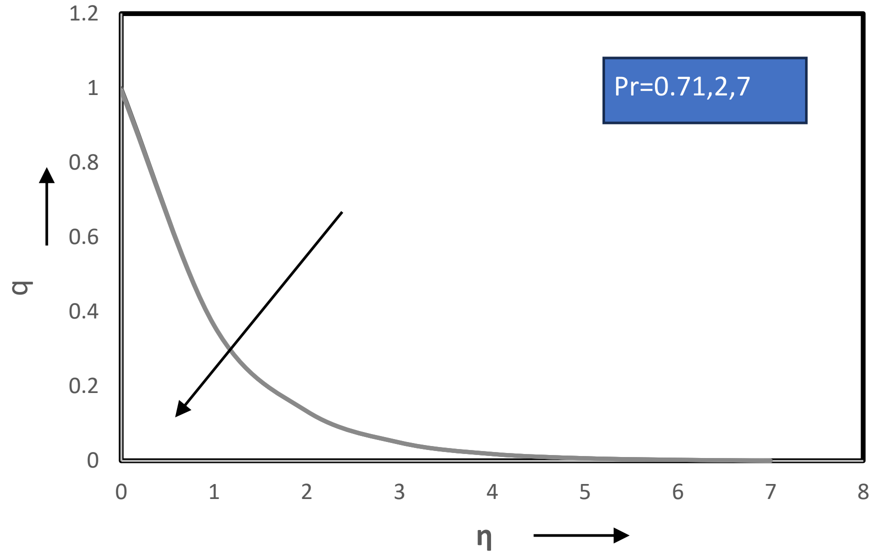

Figure 4: Variation of velocity for Pr

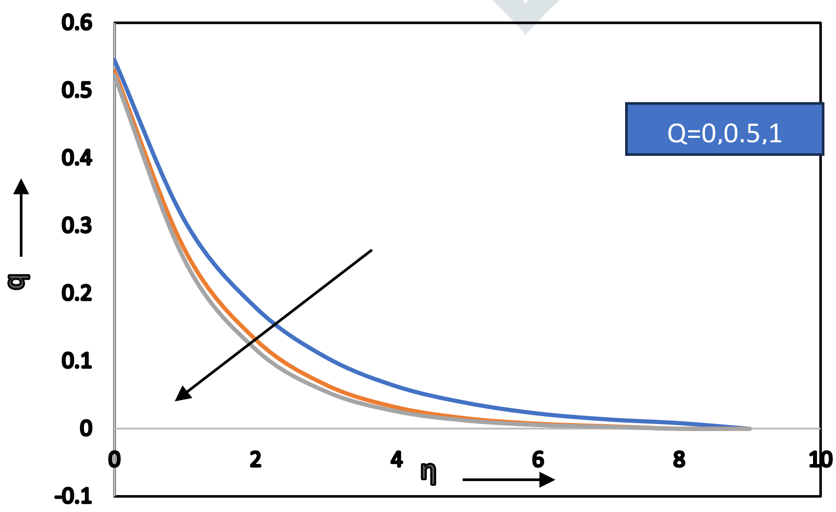

Figure 5: Variation of velocity for Q.

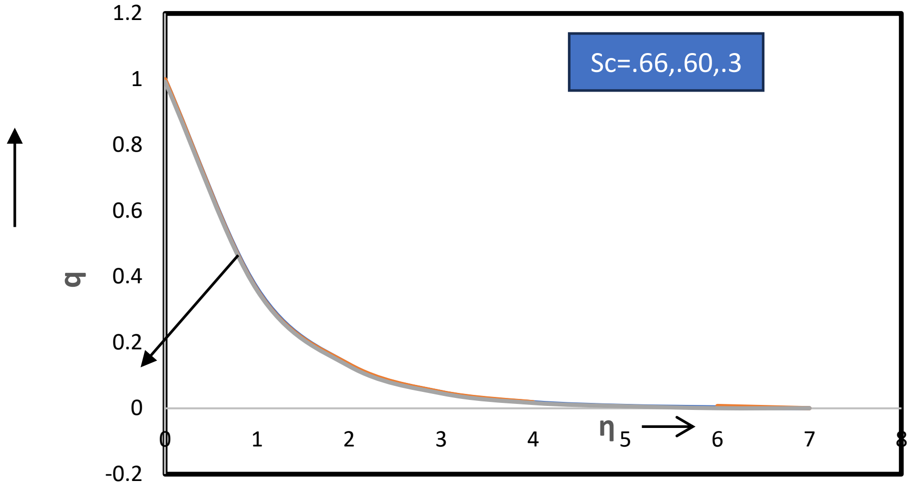

Fig 6: Variation of velocity for Sc

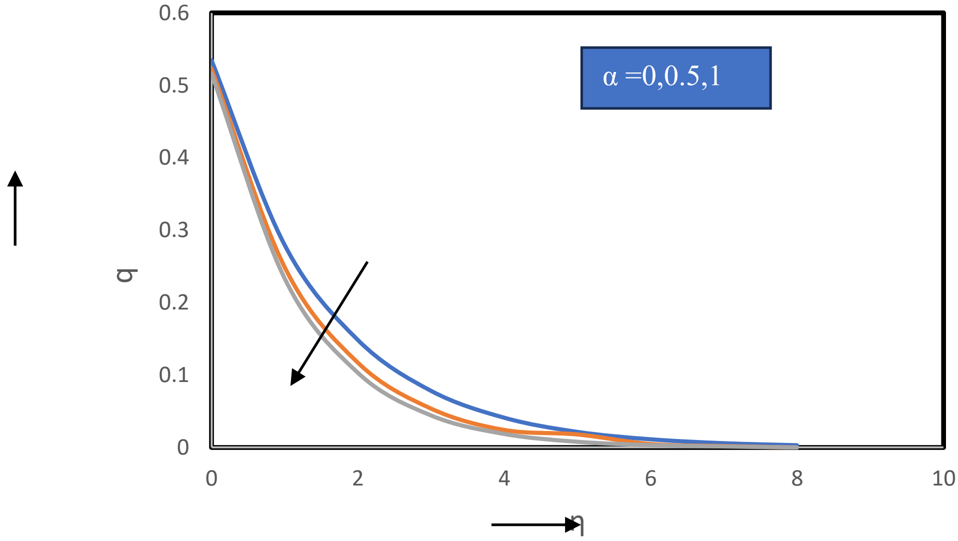

Fig 7: variation of velocity for α

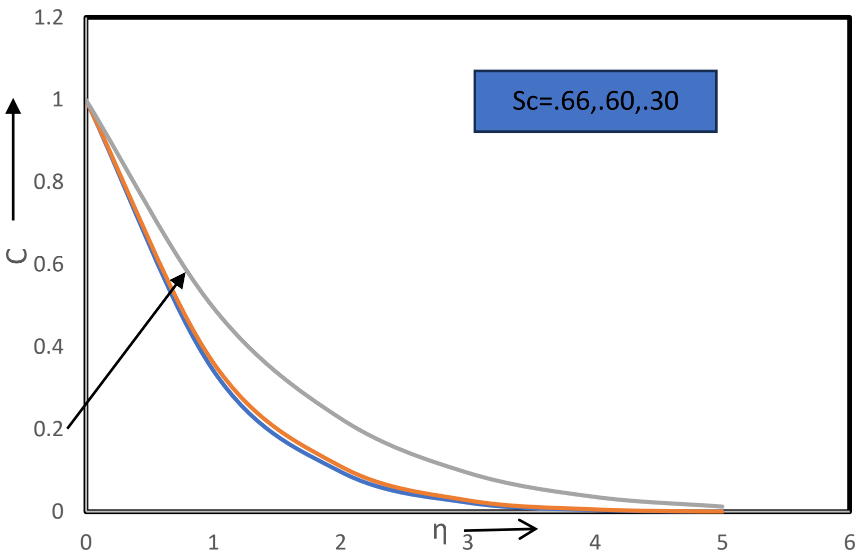

Fig 8: concentration profile for Sc.

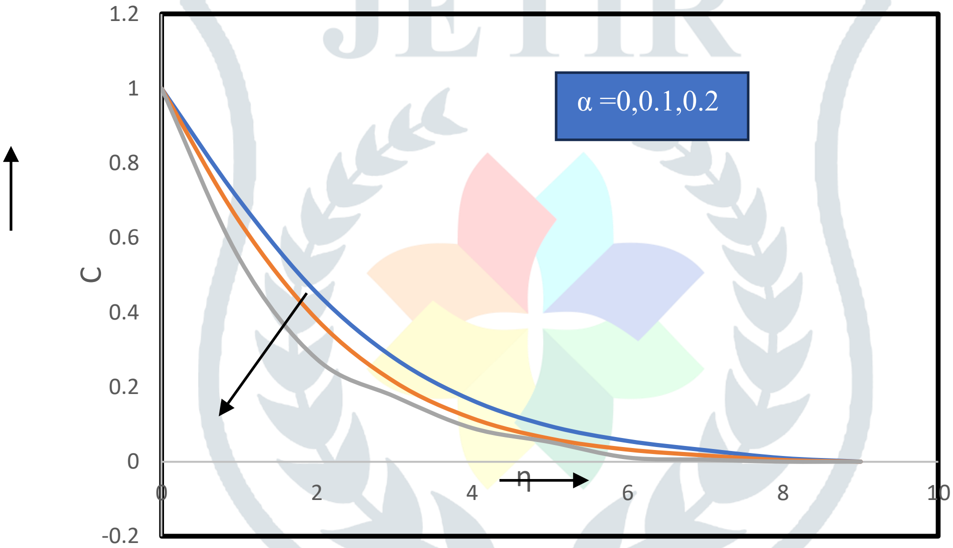

Fig 9: Variation of concentration for α

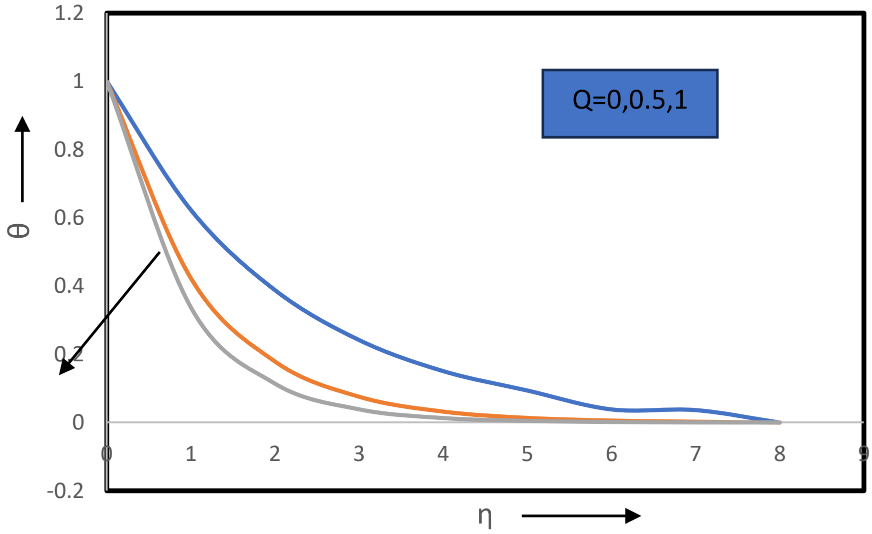

Fig 10: Variation of temperature for Q

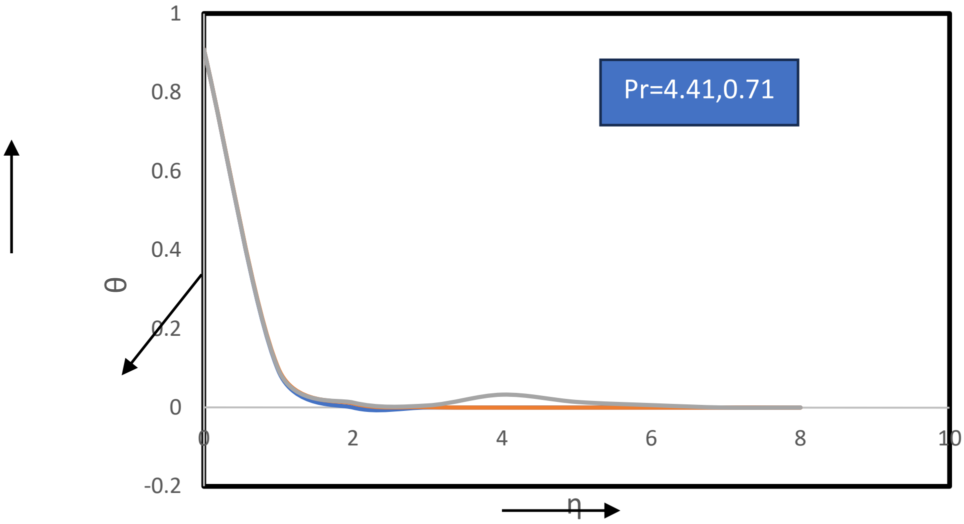

Fig 11: Variation of temperature for Pr

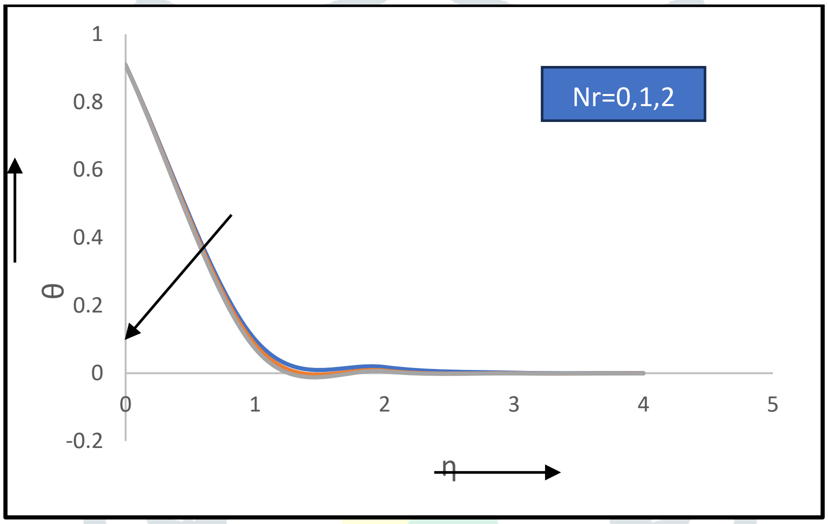

Fig 12: Variation of temperature for Nr

Table 1: Effect of parameter Pr, Nr, Q, ω on $NuRe_x^{-1}$

Pr	Nr	Q	ω	$NuRe_x^{-1}$
0.25	1.0	0.5	0.01	-0.5063
.71	1.0	0.5	0.01	-0.7081
7	1.0	0.5	0.01	-3.5700
.71	1.2	0.5	0.01	-0.6647
.71	1.4	0.5	0.01	-0.6277
.71	1.0	1.0	0.01	-0.9065
.71	1.0	1.5	0.01	-1.0615
.71	1.0	0.5	0.02	-0.7081
.71	1.0	0.5	0.03	-0.7081

Table 2: Effect of parameter α, ω, Sc on $ShRue_x^{-1}$

α	ω	Sc	$ShRe_x^{-1}$
0	0.01	0.66	-0.6600
0.1	0.01	0.66	-0.6959
0.2	0.01	0.66	-0.7286
0.1	0.02	0.66	-0.6959
0.1	0.03	0.66	-0.6959
0.1	0.01	0.60	-0.6391
0.1	0.01	0.30	-0.3679

3. CONCLUSION

A numerical analysis of oscillatory MHD flow over a vertical plate with first-order slip has been presented. The major conclusions are:

- Magnetic and heat-absorption effects suppress velocity and reduce the momentum boundary-layer thickness.
- Increasing thermal radiation elevates the temperature and thickens the thermal boundary layer.
- Higher (Pr) enhances surface heat transfer owing to reduced thermal diffusivity.
- Increasing (α) decreases species concentration, whereas higher (Sc) reduces concentration and enhances surface mass transfer.
- Thermal radiation reduces the wall heat-transfer rate, while (Pr) and heat absorption significantly influence thermal transport.
- Rotation has a negligible effect on heat and mass transfer within the investigated range.
- Increasing (Pr) from 0.25 to 7 enhances the reduced Nusselt number, whereas increasing (Nr) from 1.0 to 1.4 reduces it.
- Increasing (α) from 0 to 0.2 and increasing (Sc) enhance the magnitude of the Sherwood number, indicating stronger surface mass transfer.
- Variation of (ω) from 0.01 to 0.03 produces negligible changes in the Sherwood number.

Overall, the results confirm that magnetic interaction, thermal radiation, heat absorption, chemical reaction, diffusion, rotation, and wall slip collectively govern the momentum, heat, and mass-transfer characteristics of the flow

ACKNOWLEDGEMENTS
The authors gratefully acknowledge the reviewers for their careful evaluation, valuable comments, and constructive suggestions, which greatly enhanced the scientific quality and clarity of this manuscript. One of the authors, Babul Chandra Das, extends his heartfelt thanks to Mrs. Jonti Das for her kind assistance in the English language editing and proofreading of the manuscript.

NOMENCLATURE

C	Species concentration
C_f	Local skin friction coefficient
c^*	Concentration of species in the fluid
C_∞^*	Ambient concentration
c_p	Specific heat at a constant pressure.
D_M	Mass diffusivity
G	Acceleration due to gravity
G_r	Grashof number for heat transfer
G_c	Grashof mass transfer
j	Current density
K_c^*	Chemical reaction rate constant
K_C	Chemical reaction rate
m	Hall current parameter
M	Magnetic parameter

Nu_x Local Nusselt number
Nr Radiation parameter
Pr Prandtl number
Q Absorption parameter
Q_0 Heat absorption coefficient
q_r Relative heat flux
R Rational parameter
Sc Schmidt number
T_∞^* Ambient temperature
T^* Fluid temperature
T_∞ Ambient temperature
U_p, W_p Dimensionless particle velocity component
u, v, w Dimensionless velocity component
u^*, v^*, w^* Primary, transverse, secondary velocity component
v_0 Section velocity
y^* Coordinate normal to the surface

Greek Symbols
α Chemical reaction parameter
β_0 Uniform magnetic field
β_T Thermal expansion coefficient
γ Kinematic viscosity
ρ Fluid density
Ω Angular velocity
θ Dimensionless temperature
η Dimensional spatial coordinate
σ Electrical conductivity
Subscript
ω Condition at the wall
∞ Free stream function

References

1. Das, U. J., & Das, M. (2021). *Unsteady MHD rotating and chemically reacting fluid flow over an oscillating vertical surface in a Darcian porous regime*. Frontiers in Heat and Mass Transfer, 17, 1–8. DOI: 10.5098/hmt.17.18

2. Singh, J. K., Rohidas, P., Joshi, N., & Begum, S. G. *Influence of Hall and ion-slip currents on unsteady MHD free convective flow of a rotating fluid past an oscillating vertical plate*. International Journal of Heat and Technology, 35, 37–52. DOI: 10.18280/ijht.350106

3. Ahmed, S. — *Hartmann Newtonian radiating MHD flow for a rotating vertical porous channel immersed in a Darcian porous regime: An exact solution*. International Journal of Numerical Methods for Heat & Fluid Flow, 24 (2014), 1454–1470. DOI: 10.1108/HFF-04-2013-0113.

4. Ganesh, N. V., Al-Mdallal, Q., & Kalaivananc, R. (2021). *Exact solution for heat transport of Newtonian fluid with quadratic order thermal slip in a porous medium*. Advances in the Theory of Nonlinear Analysis and its Application, 5(1).

5. Jasim, A. M. (2020). *Analytical approximation of the first grade MHD squeezing fluid flow with slip boundary condition using a new iterative method*. Heat Transfer. DOI: 10.1002/htj.21901

6. Pal, D. & Talukdar, B. — *Numerical/Laplace transform analysis for MHD radiating heat/mass transport in a Darcian porous regime bounded by an oscillating vertical surface*. Alexandria Engineering Journal, 54 (2015), 45–54. DOI: 10.1016/j.aej.2014.11.006.

7. Singh, J. K., Rohidas, P., Joshi, N., & Begum, S. G. *Influence of Hall and ion-slip currents on unsteady MHD free convective flow of a rotating fluid past an oscillating vertical plate*. International Journal of Heat and Technology, 35, 37–

52.
DOI: 10.18280/ijht.350106

8. Ganesh, N. V., Al-Mdallal, Q., & Kalaivananc, R. (2021). *Exact solution for heat transport of Newtonian fluid with quadratic order thermal slip in a porous medium*. Advances in the Theory of Nonlinear Analysis and its Application, 5(1). https://doi.org/10.17762/atnaa.v5.i1.180

9. Jasim, A. M. (2020). *Analytical approximation of the first grade MHD squeezing fluid flow with slip boundary condition using a new iterative method*. Heat Transfer. DOI: 10.1002/htj.21901

10. Useful particularly for the mathematical treatment of MHD slip flow in a porous medium and first-order slip-type boundary conditions.

11. Sajid, M N., Ali, N., Abbas, Z., and Javed, T., Stretching flows with general slip boundary condition, International Journal of Modern Physics B, 24(30) (2010)5939-5947. https://doi.org/10.1142/S0217979210055512.

12. Nandeppanavar, M.M., Vajravelu, K., Abel, M.S., and Siddalingappa, M.N., Second order slip flow and heat transfer over a stretching sheet with non-linear Navier boundary condition, International Journal of Thermal Sciences, 58 (2012)143-150. https://doi.org/10.1016/J.IJTHERMALSCI.2012.02.019.

13. Turkyilmazoglu, M., Heat and mass transfer of MHD second order slip flow. Computers & Fluids, 71 (2013) 426-434. https://doi.org/10.1016/j.compfluid.2012.11.011

14. Liu, Y., and Guo, B., Effects of second-order slip on the ow of a fractional Maxwell MHD fluid, Journal of the Association of Arab Universities for Basic and Applied Sciences, 24 (2017) 232-241. https://doi.org/10.1016/j.jaubas.2017.04.001

15. Mabood, F., Shaq, A., Hayat, T., and Abelman, S., Radiation effects on stagnation point flow with melting heat transfer and second order slip, Results in Physics, 7 (2017) 31-42. https://doi.org/10.1016/j.rinp.2016.11.051

16. Aman, S., Al-Mdallal, Q., and Khan, I., Heat transfer and second order slip effect on MHD ow of fractional Maxwell fluid in a porous medium, Journal of King Saud University-Science, 32(1)(2020)450-458. doi:10.1016/j.jksus.2018.07.007

17. Ganesh, N.V., Al-Mdallal, Q.M., and Chamkha, A.J. A numerical investigation of Newtonian fluid flow with buoyancy, thermal slip of order two and entropy generation, Case Studies in Thermal Engineering, 13 (2019) 100376. https://www.google.com.

Appendix

$$a_1=\frac{1}{k}+\frac{i\omega}{4}+\frac{M(1-im)}{(1+m^2)},\ a_2=\frac{1}{Pr}(1+Nr),\ a_3=\frac{Q}{Pr}+\frac{i\omega}{4},\ a_4=\alpha+\frac{i\omega}{4},\ M=\frac{\sigma B_0^2}{\rho V_0^2},\ R=\frac{2\gamma\Omega}{V_0^2}$$

$$\alpha=\frac{K_c\gamma}{V_0^2},\ m_1=\frac{-1+\sqrt{4a_0a_3}}{2a_0},\ m_2=\frac{-1-\sqrt{1+4a_0a_3}}{2a_3},\ m_3=\frac{-S_c-\sqrt{S_c^2+4a_4}}{2},\ m_4=\frac{-1-\sqrt{1+4a_1}}{2}$$

$$m_5=\frac{-1+\sqrt{1+4a_1}}{2},\ D_1=\frac{-A_1Gr}{D^2+D-a_1},\ D_2=\frac{-A_2Gc}{D^2+D-a_1},\ E_1=\frac{A_3+D_1+D_2}{A},\ E_2=\frac{q_p}{A}$$

....